2011 50th IEEE Conference on Decision and Control and
European Control Conference (CDC-ECC)
Orlando, FL, USA, December 12-15, 2011

Constraint Handling within a Multi-blade Coordinate Framework of a Wind Turbine

Lars Christian Henriksen and Niels Kjølstad Poulsen and Hans Henrik Niemann

Abstract— **In this paper the control of a horizontal axis pitch controlled wind turbine using Model Predictive Control is presented. The multi-blade coordinate transformation is utilized to turn the rotating frame time-varying system description into a time-invariant fixed frame system description. Constraints in the rotating frame of reference are not easily described in the fixed frame and a Model Predictive Control formulation accommodating this problem is presented. The presented method is tested with satisfactory results in a numerical simulation.**

I. INTRODUCTION

The wind turbine shares properties with other rotating systems such as helicopters and much of the wind turbine theory originates from helicopter theory. Multi-blade coordinate (MBC) transformation also denoted the Coleman transformation [1] is a method to transform the degrees of freedom on the rotor to degrees of freedom in the fixed frame of reference.

An example could be wind shear, meaning that the wind speed near ground is lower than the wind speed at the top of the wind turbine. As the blades revolve they will alternate between high and low wind speeds in a periodic manner and the wind speed felt by each blade is sinusoidal for a linear wind shear. The MBC transformation of the wind speeds into the fixed frame results in a degree of freedom describing the average wind speed, a degree of freedom describing the wind shear and a degree of freedom describing if the wind speeds are higher at on side of the rotor compared to the other side. For linear wind shear the MBC transformed quantities are constant, turning a time-varying degree of freedom into a time-invariant degree of freedom.

Another example could be that as the blades revolve they will apply a force at the root of the blade on the tower side-side degree of freedom, but depending on the azimuthal position of the blade, the force will be transferred to the tower in different ways, resulting in a time-varying system. Both examples can be seen in Fig. 1. The relationship between the variables in the rotating frame and in the fixed frame can be seen in Fig. 2. The MBC transformation applied to the wind turbine transforms all these periodically time-varying degrees of freedom and system equations into a time-invariant system. MBC for dynamical analysis of the wind turbine is a strong tool and e.g. [2] and [3] discusses the subject in much greater depth.

The benefit of MBC when in used control of wind turbines have previously been documented by e.g. [4]. Another use of MBC in the field of wind turbine control is found in [5] where a wind turbulence model in the fixed frame of reference is also derived. Common for MBC-based control algorithms is the use of individual pitch of the blades facilitated by the MBC formulation to mitigate loads on the wind turbine caused by asymmetric loading such as wind shear.

Model Predictive Control (MPC) [6], [7] offers a systematic way to handle constraints on e.g. pitch rate of the blades. The authors have previously developed a wind turbine control framework with MPC [8] and this framework is extended to include the MBC formulation of the wind turbine in this paper. Constraints defined in the rotating frame of reference are not easily translated into the fixed frame of reference and a solution to this problem is presented in this paper.

The papers outline is as follows: The multi-blade coordinate transformation is discussed in Section II. The wind turbine model used by the model-based state estimator and state feedback control algorithms is presented in Section III. The overall controller setup and the state estimation and control algorithms are explained in Section IV. Simulation results demonstrating the constraint handling capabilities of the controller are presented in Section V. Finally, conclusions are drawn in Section VI.

II. MULTI-BLADE COORDINATE TRANSFORMATION

In this section the fundamentals of the multi-blade coordinate (MBC) transformation are introduced in the first subsection. Following is a subsection describing how the MBC transformation is applied on the state space model.

A. MBC fundamentals

The MBC transformation enables the transformation from a rotating frame of reference to a fixed frame of reference. The azimuth angle ϕ_i of blades $i = 1, \ldots, n_{blades}$, assuming constant rotor speed Ω and equal angular spacing between the blades, is given by

$$\phi_i = \phi_0 + \Omega t - (i-1)\pi/n_{blades} \tag{1}$$

and renders the MBC transformation a function of time t rather than the azimuth angle ϕ. The azimuth angles can be combined in a vector, which for a 3-bladed rotor is $\boldsymbol{\phi} = [\phi_1 \ \phi_2 \ \phi_3]^T$. The temporal argument of states and

This work is supported by the CASED Project funded by grant DSF-09-063197 of the Danish Council for Strategic Research.

L. C. Henriksen is with DTU Informatics, Technical University of Denmark DK-2800 Kgs. Lyngby, Denmark larh@imm.dtu.dk

N. K. Poulsen is with DTU Informatics, Technical University of Denmark DK-2800 Kgs. Lyngby, Denmark nkp@imm.dtu.dk

H. H. Niemann is with DTU Electro, Technical University of Denmark DK-2800 Kgs. Lyngby, Denmark hhn@elektro.dtu.dk

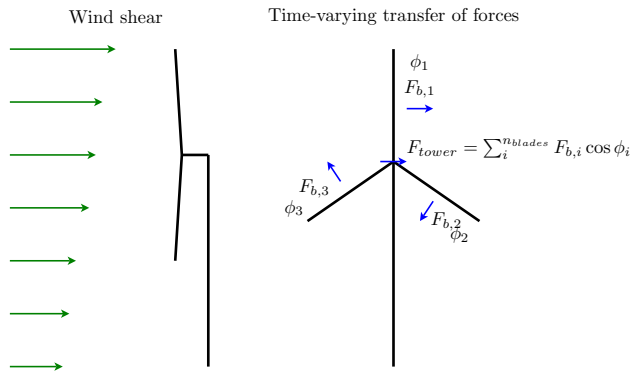

Fig. 1. Examples of time-varying quantities on a wind turbine. To the left: The wind shear means that the revolving blades will be subjected to periodically varying loading conditions. To the right: The forces transferred from the blades to the tower side-side degree of freedom are transferred differently depending on the azimuth angle ψ_i of the individual blade.

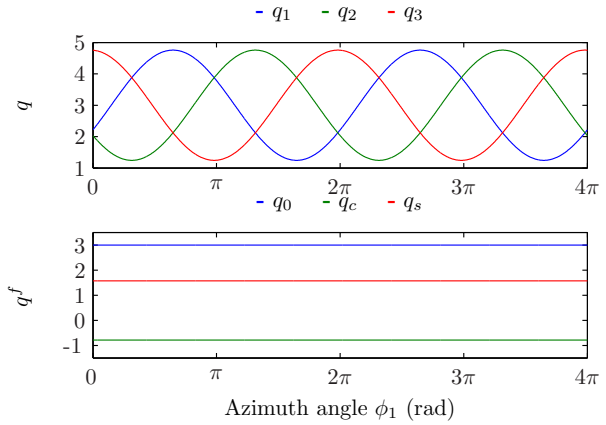

Fig. 2. Degrees of freedom in rotating frame of reference $\boldsymbol{q}$ transformed to the fixed frame of reference $\boldsymbol{q^f}$ using the multi-blade coordinate transformation.

transformation matrices in the following has been omitted to simplify notation. The rotating frame coordinates $\boldsymbol{q}$ and the fixed frame coordinates $\boldsymbol{q^f}$ and their temporal derivatives have the following relationship

$$\boldsymbol{q} = \mathbf{M}^{-1}\boldsymbol{q^f} \tag{2a}$$
$$\dot{\boldsymbol{q}} = \dot{\mathbf{M}}^{-1}\boldsymbol{q^f} + \mathbf{M}^{-1}\dot{\boldsymbol{q}}^{\boldsymbol{f}} \tag{2b}$$
$$\ddot{\boldsymbol{q}} = \ddot{\mathbf{M}}^{-1}\boldsymbol{q^f} + 2\dot{\mathbf{M}}^{-1}\dot{\boldsymbol{q}}^{\boldsymbol{f}} + \mathbf{M}^{-1}\ddot{\boldsymbol{q}}^{\boldsymbol{f}} \tag{2c}$$

where (2a) is the base transformation and (2b) is derived from $\dot{\boldsymbol{q}} = \frac{d}{dt}(\mathbf{M}^{-1}\boldsymbol{q^f})$ and 2c from $\ddot{\boldsymbol{q}} = \frac{d}{dt}(\dot{\mathbf{M}}^{-1}\boldsymbol{q^f} + \mathbf{M}^{-1}\dot{\boldsymbol{q}}^{\boldsymbol{f}})$. The inverse transformations are given by

$$\boldsymbol{q^f} = \mathbf{M}\boldsymbol{q} \tag{3a}$$
$$\dot{\boldsymbol{q}}^{\boldsymbol{f}} = \tfrac{2}{3}\dot{\mathbf{M}}^{-T}\boldsymbol{q} + \mathbf{M}\dot{\boldsymbol{q}} \tag{3b}$$
$$\ddot{\boldsymbol{q}}^{\boldsymbol{f}} = \tfrac{2}{3}\ddot{\mathbf{M}}^{-T}\boldsymbol{q} + \tfrac{4}{3}\dot{\mathbf{M}}^{-T}\dot{\boldsymbol{q}} + \mathbf{M}\ddot{\boldsymbol{q}} \tag{3c}$$

The MBC transformation matrices are

$$\mathbf{M} = \begin{bmatrix} \frac{1}{3}\mathbf{1}^T \\ \frac{2}{3}\cos\boldsymbol{\phi}^T \\ \frac{2}{3}\sin\boldsymbol{\phi}^T \end{bmatrix}, \quad \mathbf{M}^{-1} = \begin{bmatrix} \mathbf{1}^T \\ \cos\boldsymbol{\phi}^T \\ \sin\boldsymbol{\phi}^T \end{bmatrix}^T,$$

$$\dot{\mathbf{M}}^{-1} = \Omega \begin{bmatrix} \mathbf{0}^T \\ -\sin\boldsymbol{\phi}^T \\ \cos\boldsymbol{\phi}^T \end{bmatrix}^T \text{ and } \ddot{\mathbf{M}}^{-1} = \Omega^2 \begin{bmatrix} \mathbf{0}^T \\ -\cos\boldsymbol{\phi}^T \\ -\sin\boldsymbol{\phi}^T \end{bmatrix}^T$$

where $\mathbf{1} = [1\ 1\ 1]^T$ and $\cos\boldsymbol{\phi} = [\cos\phi_1\ \ \cos\phi_2\ \ \cos\phi_3]^T$ etc.

B. The MBC transformation applied on a state space model

A dynamic system in state space form can be expressed by an nonlinear ordinary differential equation vector function and a vector output function as

$$\dot{\boldsymbol{x}}(t) = \boldsymbol{f}(\boldsymbol{x}(t), \boldsymbol{u}(t), t) \tag{4a}$$
$$\boldsymbol{y}(t) = \boldsymbol{g}(\boldsymbol{x}(t), \boldsymbol{u}(t), t) \tag{4b}$$

where states $\boldsymbol{x}$, inputs $\boldsymbol{u}$, outputs $\boldsymbol{y}$ and the vector functions $\boldsymbol{f}$ and $\boldsymbol{g}$ are all functions of time. In the following, the temporal arguments of states, inputs and outputs and vector functions have been omitted to simplify notation.

First order Taylor expansion around the linearization $(\bar{\boldsymbol{x}}, \bar{\boldsymbol{u}})$ yields

$$\dot{\boldsymbol{x}} = \boldsymbol{f}(\bar{\boldsymbol{x}}, \bar{\boldsymbol{u}}) + \mathbf{A}(\boldsymbol{x} - \bar{\boldsymbol{x}}) + \mathbf{B}(\boldsymbol{u} - \bar{\boldsymbol{u}}) \tag{5a}$$
$$\boldsymbol{y} = \boldsymbol{g}(\bar{\boldsymbol{x}}, \bar{\boldsymbol{u}}) + \mathbf{C}(\boldsymbol{x} - \bar{\boldsymbol{x}}) + \mathbf{D}(\boldsymbol{u} - \bar{\boldsymbol{u}}) \tag{5b}$$

where the system matrices $(\mathbf{A}, \mathbf{B}, \mathbf{C}, \mathbf{D})$ are functions of time. The linearization can be rewritten to

$$\dot{\boldsymbol{x}} = \mathbf{A}\boldsymbol{x} + \mathbf{B}\boldsymbol{u} + \boldsymbol{\delta}, \quad \boldsymbol{\delta} = \boldsymbol{f}(\bar{\boldsymbol{x}}, \bar{\boldsymbol{u}}) - \mathbf{A}\bar{\boldsymbol{x}} - \mathbf{B}\bar{\boldsymbol{u}} \tag{6a}$$
$$\boldsymbol{y} = \mathbf{C}\boldsymbol{x} + \mathbf{D}\boldsymbol{u} + \boldsymbol{\gamma}, \quad \boldsymbol{\gamma} = \boldsymbol{g}(\bar{\boldsymbol{x}}, \bar{\boldsymbol{u}}) - \mathbf{C}\bar{\boldsymbol{x}} - \mathbf{D}\bar{\boldsymbol{u}} \tag{6b}$$

for typical linear control theory the pair $(\bar{\boldsymbol{x}}, \bar{\boldsymbol{u}})$ is chosen to be an equilibrium point (such that $\mathbf{0} = \boldsymbol{f}(\bar{\boldsymbol{x}}, \bar{\boldsymbol{u}})$), but the theory is also valid for other choices of $(\bar{\boldsymbol{x}}, \bar{\boldsymbol{u}})$.

A state space system description of a wind turbine with fixed frame degrees of freedom $\boldsymbol{x_1}$ e.g. tower fore-aft, rotor speed etc and rotating frame degrees of freedom $\boldsymbol{x_2} = [\boldsymbol{q}\ \dot{\boldsymbol{q}}]$ such as blade pitch angle $\boldsymbol{q}$ and blade pitch $\dot{\boldsymbol{q}}$. Fixed frame inputs $\boldsymbol{u_1}$ such as generator torque and rotating frame inputs $\boldsymbol{u_2}$ such as pitch angle reference

$$\boldsymbol{x} = \begin{bmatrix} \boldsymbol{x_1} \\ \boldsymbol{q} \\ \dot{\boldsymbol{q}} \end{bmatrix} \quad \boldsymbol{u} = \begin{bmatrix} \boldsymbol{u_1} \\ \boldsymbol{u_2} \end{bmatrix} \quad \boldsymbol{y} = \begin{bmatrix} \boldsymbol{x_1} \\ \dot{\boldsymbol{x}}_1 \\ \boldsymbol{q} \\ \dot{\boldsymbol{q}} \\ \ddot{\boldsymbol{q}} \end{bmatrix} \tag{7}$$

and outputs containing both rotating and fixed frame quantities.

The time-varying combined fixed and rotating frame system (7) can be transformed to a fixed frame time-invariant system where the states, inputs and outputs are transformed to the fixed frame of reference

$$\boldsymbol{x^f} = \mathbf{M_x}\boldsymbol{x} \text{ and } \boldsymbol{u^f} = \mathbf{M_u}\boldsymbol{u} \text{ and } \boldsymbol{y^f} = \mathbf{M_y}\boldsymbol{y}. \tag{8}$$

The MBC transformations gives the fixed frame system equations

$$\dot{\boldsymbol{x}}^{\boldsymbol{f}} = \mathbf{A}^{\mathbf{f}}\boldsymbol{x}^{\boldsymbol{f}} + \mathbf{B}^{\mathbf{f}}\boldsymbol{u}^{\boldsymbol{f}} + \delta^{\mathbf{f}} \tag{9a}$$

$$\boldsymbol{y}^{\boldsymbol{f}} = \mathbf{C}^{\mathbf{f}}\boldsymbol{x}^{\boldsymbol{f}} + \mathbf{D}^{\mathbf{f}}\boldsymbol{u}^{\boldsymbol{f}} + \boldsymbol{\gamma}^{\boldsymbol{f}} \tag{9b}$$

where

$$\begin{aligned} \mathbf{A}^{\mathbf{f}} &= \tilde{\mathbf{M}}_{\mathbf{x}}(\mathbf{A}\mathbf{M}_{\mathbf{x}}^{-1} - \dot{\mathbf{M}}_{\mathbf{x}}^{-1}), & \mathbf{C}^{\mathbf{f}} &= \mathbf{M}_{\mathbf{y}}\mathbf{C}\mathbf{M}_{\mathbf{x}}^{-1}, \\ \mathbf{B}^{\mathbf{f}} &= \tilde{\mathbf{M}}_{\mathbf{x}}\mathbf{B}\mathbf{M}_{\mathbf{u}}^{-1}, & \mathbf{D}^{\mathbf{f}} &= \mathbf{M}_{\mathbf{y}}\mathbf{D}\mathbf{M}_{\mathbf{u}}^{-1}, \\ \boldsymbol{\delta}^{\boldsymbol{f}} &= \tilde{\mathbf{M}}_{\mathbf{x}}\boldsymbol{\delta}, & \boldsymbol{\gamma}^{\boldsymbol{f}} &= \mathbf{M}_{\mathbf{y}}\boldsymbol{\gamma}. \end{aligned}$$

The system matrices $(\mathbf{A}^{\mathbf{f}}, \mathbf{B}^{\mathbf{f}}, \mathbf{C}^{\mathbf{f}}, \mathbf{D}^{\mathbf{f}})$ are time-invariant, as are the residual vectors $(\boldsymbol{\delta}^{\boldsymbol{f}}, \boldsymbol{\gamma}^{\boldsymbol{f}})$ when rotating frame variables have been averaged in the linearization point

$$\bar{\boldsymbol{q}} = \text{mean}(\boldsymbol{q}) \text{ and } \bar{\dot{\boldsymbol{q}}} = \text{mean}(\dot{\boldsymbol{q}}).$$

The state equation MBC transformation matrices are

$$\tilde{\mathbf{M}}_{\mathbf{x}} = \begin{bmatrix} \mathbf{I} & & \\ & \mathbf{M} & \\ & & \mathbf{M} \end{bmatrix}, \quad \mathbf{M}_{\mathbf{x}}^{-1} = \begin{bmatrix} \mathbf{I} & & \\ & \mathbf{M}^{-1} & \\ & \dot{\mathbf{M}}^{-1} & \mathbf{M}^{-1} \end{bmatrix}$$

and

$$\dot{\mathbf{M}}_{\mathbf{x}}^{-1} = \begin{bmatrix} \mathbf{0} & & \\ & \dot{\mathbf{M}}^{-1} & \\ & \ddot{\mathbf{M}}^{-1} & 2\dot{\mathbf{M}}^{-1} \end{bmatrix}$$

For control signals and outputs the matrices are

$$\mathbf{M}_{\mathbf{u}} = \begin{bmatrix} \mathbf{I} & \\ & \mathbf{M} \end{bmatrix} \text{ and } \mathbf{M}_{\mathbf{y}} = \begin{bmatrix} \mathbf{I} & & & & \\ & \mathbf{I} & & & \\ & & \mathbf{M} & & \\ & & & \mathbf{M} & \\ & & & & \mathbf{M} \end{bmatrix}$$

The nonlinear time discrete state progress equation

$$\boldsymbol{x}_{k+1}^{\boldsymbol{f}} = \underline{\boldsymbol{f}}^{\boldsymbol{f}}(\boldsymbol{x}_k^{\boldsymbol{f}}, \boldsymbol{u}_k^{\boldsymbol{f}}) = \boldsymbol{x}_k^{\boldsymbol{f}} + \int_{t_k}^{t_{k+1}} \dot{\boldsymbol{x}}^{\boldsymbol{f}}(\tau)d\tau \tag{10}$$

used in Section IV can be approximated by a linear description

$$\begin{aligned} \boldsymbol{x}_{k+1}^{\boldsymbol{f}} &= \underline{\mathbf{A}}^{\mathbf{f}}\boldsymbol{x}_k^{\boldsymbol{f}} + \underline{\mathbf{B}}^{\mathbf{f}}\boldsymbol{u}_k^{\boldsymbol{f}} + \underline{\boldsymbol{\delta}}^{\boldsymbol{f}}, \\ \underline{\boldsymbol{\delta}}^{\boldsymbol{f}} &= \underline{\boldsymbol{f}}^{\boldsymbol{f}}(\bar{\boldsymbol{x}}^{\boldsymbol{f}}, \bar{\boldsymbol{u}}^{\boldsymbol{f}}) - \underline{\mathbf{A}}^{\mathbf{f}}\bar{\boldsymbol{x}}^{\boldsymbol{f}} - \underline{\mathbf{B}}^{\mathbf{f}}\bar{\boldsymbol{u}}^{\boldsymbol{f}} \end{aligned} \tag{11}$$

and [9] gives further details regarding implementation.

III. WIND TURBINE MODEL

The governing equations constituting the control design model used in Section IV are presented in this section.

The aerodynamic torques and thrust forces of blades $i = 1, 2, 3$

$$Q_i(\Omega, V_{rel,i}, \theta_i, v_{n,i}) \text{ and } T_i(\Omega, V_{rel,i}, \theta_i, v_{n,i}) \tag{12}$$

are, respectively, functions of rotor speed Ω, blade pitch angle θ_i, blade-specific relative wind speed $V_{rel,i}$ and blade-specific normal induced wind speed $\bar{v}_{n,i}$. The temporal dynamics of the blade-specific normal induced wind speed are governed by first order ordinary differential equations

$$\bar{v}_{n,i} = \frac{1}{\tau_{n,is+1}} V_{rel,i}\bar{a}_n^{QS}(V_{rel,i}, \Omega, \theta_i) \tag{13}$$

where the quasi-steady induction factor lookup table $\bar{a}_n^{QS}$ is calculated offline using blade element momentum theory [8]. The relative wind speed average for each blade due to the velocity of nacelle displacement $\dot{\psi}_t$ is given by

$$V_{rel,i} = V_i - \dot{\psi}_t \tag{14}$$

where the effective wind speed V_i of each blade is given by the wind model presented in the next paragraph. The blade-specific wind speed are gathered in a vector $\boldsymbol{V} = [V_1\ V_2\ V_3]^T$ which are related to the fixed frame wind speed vector $\boldsymbol{V}^f = [V_0^f\ V_c^f\ V_s^f]^T$ via the MBC transform

$$\boldsymbol{V} = \mathbf{M}^{-1}\boldsymbol{V}^{\boldsymbol{f}}. \tag{15}$$

In [5] it has been shown how to derive the wind turbulence model in fixed frame coordinates. The fixed-frame wind model for an isotropic rotor is a sum of harmonic components with peak frequencies which are multiples of of the rotor speed multiplied with the number of blades

$$f_n = n3\Omega/(2\pi). \tag{16}$$

In the present work the harmonic components are approximated by second order ordinary differential equations and only the first harmonic component (n=1) is included in the model. The damped frequency of the model is $\omega_d = 3\Omega$, giving a natural frequency $\omega_f = \omega_d/(\sqrt{1-\zeta_f^2})$. The fixed frame wind speeds $\boldsymbol{V}^{\boldsymbol{f}}$ are the sum of the steady state fixed frame wind speeds $\bar{\boldsymbol{V}}^{\boldsymbol{f}}$ and the dynamic fixed frame wind speeds $\boldsymbol{\Delta}\bar{\boldsymbol{V}}^{\boldsymbol{f}}$ given by

$$\Delta\ddot{V}_j^f + 2\zeta_f\omega_f\Delta\dot{V}_j^f + \omega_f^2\Delta V_j^f = \omega_f^2 w_j \tag{17}$$

for $j = (0, c, s)$ and where is w_j zero-mean Gaussian distributed noise with variance $\sigma_{f,j}^2$. The parameter vector $\bar{\boldsymbol{V}}$ is updated in each sample and is governed by first order ordinary differential equations

$$\tau\dot{\bar{V}}_j^f + \bar{V}_j^f = \bar{V}_j^f + \Delta V_j^f, \quad j = (0, c, s) \tag{18}$$

driven by the wind speeds estimated by the extended Kalman filter presented in next section.

The drive-train connects the rotor to the generator through a low speed shaft, a gearbox and a high speed shaft. The drive-train flexibility is modeled in the low speed shaft coordinate system

$$I_r\ddot{\phi}_r + D_s\dot{\phi}_\Delta + K_s\phi_\Delta = Q_1 + Q_2 + Q_3 \tag{19a}$$

$$I_g N_g^2 \frac{\ddot{\phi}_g}{N_g} - D_s\dot{\phi}_\Delta - K_s\phi_\Delta = -Q_g N_g \tag{19b}$$

where N_g is the gear ratio, I_r and I_g are the moments of inertia of the rotor and generator, K_s and D_s are the spring and damping constants. It should also be mentioned that the following definitions are introduced: $\dot{\phi}_r \equiv \Omega$ is rotor speed,

$\dot{\phi}_g \equiv \Omega_g$ is generator speed and $\phi_\Delta \equiv \phi_r - \frac{\phi_g}{N_g}$ is the angular torsion of the drive-shaft in the low speed shaft coordinate system. Another significant model component is the fore-aft motion of the tower

$$M_t\ddot{\psi}_t + D_t\dot{\psi}_t + K_t\psi_t = T_1 + T_2 + T_3 \tag{20}$$

where ψ_t denotes the nacelle displacement in the fore-aft direction and is positive in the wind direction, M_t denotes the tower, rotor and nacelle equivalent mass and K_t and D_t denotes the tower spring and damping constants.

The actuators are assumed linear under the assumption that a low level controller, e.g. PID or some type of nonlinear controller, is operating in closed loop with the actuator mechanics. The closed loop actuator is described with second order dynamics, an approximation which under the proper conditions can be justified

$$\ddot{\theta}_i + 2\zeta_\theta\omega_\theta\dot{\theta}_i + \omega_\theta^2\theta_i = \omega_\theta^2\theta_{i,ref} \tag{21a}$$

subject to

$$\begin{bmatrix}\theta_{min}\\ \dot{\theta}_{min}\end{bmatrix} \leq \begin{bmatrix}\theta_i\\ \dot{\theta}_i\end{bmatrix} \leq \begin{bmatrix}\theta_{max}\\ \dot{\theta}_{max}\end{bmatrix} \tag{21b}$$

where ω_θ and ζ_θ are the natural frequency and damping ratio of the actuator and θ_{ref} is the reference signal from the controller. The generator torque actuator is assumed to be described with first order dynamics

$$\dot{Q}_g + \tau_g^{-1}Q_g = \tau_g^{-1}Q_{g_{ref}} \tag{22a}$$

subject to

$$\begin{bmatrix}Q_{g,min}\\ \dot{Q}_{g,min}\end{bmatrix} \leq \begin{bmatrix}Q_g\\ \dot{Q}_g\end{bmatrix} \leq \begin{bmatrix}Q_{g,max}\\ \dot{Q}_{g,max}\end{bmatrix} \tag{22b}$$

where τ_g is the time constant of the generator torque actuator and $Q_{g_{ref}}$ is the reference signal from the controller.

IV. CONTROLLER

In the following the general control setup is explained as well as the underlying model-based state estimation and control methods.

A. Controller Setup

The wind turbine can operate in either partial or full load conditions. Partial load operation means that the wind speed is lower than the rated wind speed and the wind turbine is not able to reach its nominal power production. In partial load operation the control objective is to maximize power capture. Full load operation means that the wind speed is above the rated wind speed and that the wind turbine is able to produce its nominal power. In full load operation the control objective is to keep power production at its nominal level.

In the following, several different outputs used by the control framework will be presented. The generic output $\boldsymbol{y}$ contains the following specific subsets of outputs: $\boldsymbol{y_m}$ measured outputs used by the extended Kalman Filter. The remaining outputs are used by the Model Predictive Control algorithm: $\boldsymbol{y_r}$ outputs to track a reference value e.g. generator speed Ω_g and power P_{ge}. $\boldsymbol{y_z}$ outputs which should be minimized by the controller e.g. pitch rate $\dot{\theta}$, tower fore-aft rate $\dot{\psi}_t$ etc. $\boldsymbol{y_s}$ outputs which are subject to soft constraints e.g. pitch rate $\dot{\theta}$. $\boldsymbol{y_h}$ outputs which are subject to hard constraints e.g. pitch reference θ_{ref}. Soft constraints are necessary to ensure feasibility of the model predictive control problem when plant and model does not match exactly due to e.g. parametric uncertainties, noise etc.

Depending on whether the wind turbine operate in partial or full load the control objectives change and values and weights for the various outputs of the controller change accordingly. The control framework setup can be seen in Fig. 3. An extended Kalman filter has been chosen over a linear Kalman filter as the wind turbine is a highly nonlinear plant. Consequently, the model used by the MPC algorithm is re-linearized in each sample to account for the nonlinearities of the wind turbine. Further details regarding partial and full load operation and bumpless switching between the two modes of operation can be found in e.g. [8].

B. Extended Kalman Filter

The extended Kalman Filter (EKF) is used to estimate the states, as not all states are available for the the full state feedback MPC algorithm. Furthermore, the EKF can be augmented with a disturbance model to achieve offset-free control [10], [11]. Offset-free methods will not be discussed further in this paper and the reader is referred to [8] for an elaboration on the subject.

The *a posteriori* estimate of the states with the time index $k|k$, meaning estimate at time k given by the knowledge available at time k, is given by

$$\begin{aligned}\hat{\boldsymbol{x}}^{\boldsymbol{f}}_{k|k} = \hat{\boldsymbol{x}}^{\boldsymbol{f}}_{k|k-1} + \\ \mathbf{L}_k\mathbf{M}_{\mathbf{m},k}(\boldsymbol{y}_{\boldsymbol{m},i} - \boldsymbol{g}_{\boldsymbol{m}}(\mathbf{M}^{-1}_{\mathbf{x},k}\hat{\boldsymbol{x}}^{\boldsymbol{f}}_{k|k-1}, \mathbf{M}^{-1}_{\mathbf{u},k}\boldsymbol{u}^{\boldsymbol{f}}_k))\end{aligned} \tag{23}$$

Enabling an *a priori* estimate of the states with the time index $k+1|k$, meaning estimate at time $k+1$ given knowledge available at time k, given by

$$\hat{\boldsymbol{x}}^{\boldsymbol{f}}_{k+1|k} = \underline{\boldsymbol{f}}^{\boldsymbol{f}}(\hat{\boldsymbol{x}}^{\boldsymbol{f}}_{k|k}, \boldsymbol{u}^{\boldsymbol{f}}_k) \tag{24}$$

where the Kalman gain $\mathbf{L}_k$ and output error covariance $\mathbf{\Psi}_k$ are given by

$$\mathbf{L}_k = \mathbf{P}_{k|k-1}\mathbf{C}^{\mathbf{f}T}_{\mathbf{m},k|k-1}\mathbf{\Psi}^{-1}_k \text{ and} \tag{25}$$

$$\mathbf{\Psi}_k = \mathbf{C}^{\mathbf{f}}_{\mathbf{m},k|k-1}\mathbf{P}_{k|k-1}\mathbf{C}^{\mathbf{f}T}_{\mathbf{m},k|k-1} + \mathbf{R}_{\mathbf{y}}, \tag{26}$$

respectively. The Kalman gain and output error covariance matrices are updated by the discrete time recursive Riccati equation

$$\mathbf{P}_{k|k} = \mathbf{P}_{k|k-1} - \mathbf{L}_k\mathbf{C}^{\mathbf{f}}_{\mathbf{m},k|k-1}\mathbf{P}_{k|k-1} \tag{27}$$

$$\mathbf{P}_{k+1|k} = \mathbf{A}^{\mathbf{f}}_{k|k}\mathbf{P}_{k|k}\mathbf{A}^{\mathbf{f}T}_{k|k} + \mathbf{R}_{\mathbf{x}} \tag{28}$$

The state estimate used by the full-state-feedback control algorithm can either be the *a posteriori* $\hat{\boldsymbol{x}}_{k|k}$ or the *a priori* $\hat{\boldsymbol{x}}_{k|k-1}$. In this work, the latter is used, giving the computationally expensive MPC algorithm a full sample time period to compute the control signal.

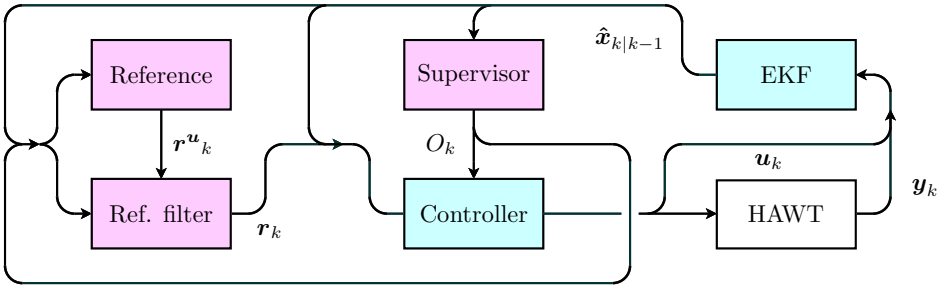

Fig. 3. Setup of the hybrid controller. An extended Kalman filter provides estimates of states used by other blocks in the diagram. Supervisor block provides partial or full load control objectives to controller depending on switching conditions. Reference and reference filter blocks provide references for the controller to track depending on whether partial or full load operation is active.

C. Model Predictive Control

The control problem, with i being the local time index within the prediction horizon, can be written as

$$\min \sum_{i=N}^{\infty} \tfrac{1}{2}\|\boldsymbol{r}^{\boldsymbol{f}} - \boldsymbol{y}^{\boldsymbol{f}}_{\boldsymbol{r},i}\|^2_{\mathbf{W_r}} + \tfrac{1}{2}\|\boldsymbol{y}^{\boldsymbol{f}}_{\boldsymbol{z},i}\|^2_{\mathbf{W_z}} + \sum_{i=0}^{N-1} \tfrac{1}{2}\|\boldsymbol{r}^{\boldsymbol{f}} - \boldsymbol{y}^{\boldsymbol{f}}_{\boldsymbol{r},i}\|^2_{\mathbf{W_r}} + \tfrac{1}{2}\|\boldsymbol{y}^{\boldsymbol{f}}_{\boldsymbol{z},i}\|^2_{\mathbf{W_z}} + \tfrac{1}{2}\|\boldsymbol{\sigma}_i\|^2_{\mathbf{W}_\sigma} \quad (29a)$$

subject to the following constraints

$$\boldsymbol{x}^{\boldsymbol{f}}_i = \hat{\boldsymbol{x}}^{\boldsymbol{f}}_{k|k-1}, \quad i = 0 \quad (29b)$$

$$\boldsymbol{x}^{\boldsymbol{f}}_{i+1} = \underline{\mathbf{A}}^{\mathbf{f}}\boldsymbol{x}^{\boldsymbol{f}}_i + \underline{\mathbf{B}}^{\mathbf{f}}\boldsymbol{u}^{\boldsymbol{f}}_i + \underline{\boldsymbol{\delta}}^{\boldsymbol{f}}, \quad i = 0 \ldots \infty \quad (29c)$$

$$\mathbf{C}_{\mathbf{h},i}\boldsymbol{x}^{\boldsymbol{f}}_i + \mathbf{D}_{\mathbf{h},i}\boldsymbol{u}^{\boldsymbol{f}}_i + \boldsymbol{\gamma}_{\boldsymbol{h}} \leq \boldsymbol{h}, \quad i = 0 \ldots N-1 \quad (29d)$$

$$\mathbf{C}_{\mathbf{s},i}\boldsymbol{x}^{\boldsymbol{f}}_i + \boldsymbol{\gamma}_{\boldsymbol{s}} - \boldsymbol{\sigma}_i \leq \boldsymbol{s}, \quad i = 1 \ldots N-1 \quad (29e)$$

$$\boldsymbol{\sigma}_i \geq \mathbf{0}, \quad i = 1 \ldots N-1 \quad (29f)$$

where $\mathbf{C}_{\mathbf{h},i} = \mathbf{C}_{\mathbf{h}}\mathbf{M}^{-1}_{\mathbf{x},i}$, $\mathbf{D}_{\mathbf{h},i} = \mathbf{D}_{\mathbf{h}}\mathbf{M}^{-1}_{\mathbf{u},i}$ and $\mathbf{C}_{\mathbf{s},i} = \mathbf{C}_{\mathbf{s}}\mathbf{M}^{-1}_{\mathbf{x},i}$ and where the re-linearized model is assumed to be linear within the prediction horizon. Further details about the RLMPC can be found in [9].

V. RESULTS

Simulations have been performed in the multi-body aero-servo-elastic software HAWC2 [12] developed by Risø DTU. The presented simulation is performed with a mean wind speed of 15 m/s and the wind turbine operate thus only in full load conditions. A power law wind shear with coefficient of 0.14 and a Mann [13] turbulence with turbulence intensity of 0.14 as well as a potential flow tower shadow model are used in the simulation. The wind turbine used in the simulation is the 5 MW reference wind turbine defined by Jonkman et al. [14].

The blades pitch individually in order to alleviate the asymmetric blade load caused wind shear etc. The blade pitch rate limits have been tightened to $\pm$ 4 deg/s to demonstrate the constraint handling capabilities of the controller.

Fig. 4 depicts the results of the simulation. Fig. 4(a) shows a point wind speed measured at the wind turbine hub. As the wind field is spatially distributed, point wind speeds at different locations in the rotor disc area are less correlated for greater distances between the point wind speeds. Accordingly, the depicted point wind speed does not give the full information about the actual conditions in which the wind turbine operate. Fig. 4(b) and 4(c) displays the controllers ability to keep the generator speed and electrical power close to their nominal values of 122.9 rad/s and 5 MW, respectively. Fig. 4(d) depicts the generator torque, which effectively is a low pass filtered inverse of the generator speed as the objective weights of the controller in the current implementation prioritizes constant power over constant generator speed. Finally, Fig. 4(e) and 4(f) shows the individual pitch activity and Fig. 4(f) documents the capability of the developed controller to honor constraints defined in the rotating frame of reference.

A close inspection of Fig. 4(f) shows that the limits are violated slightly, there are several potential causes for this: One cause could be that the numerical tolerance thresholds for convergence of the implemented quadratic programming problem solver are not small enough. Another cause could be that the pitch rate constraints are formulated as soft constraints. However, the weights on the soft constraints are so high, that the constraints act as hard constraints in most cases. Alternative simulations with even higher weights on the soft constraint violations did not show any improvement with regards to the small violations of the pitch rate limits. A third cause, and the most likely cause, could be that constraints formulated in the rotating frame of reference are subject to small errors, when transformed to fixed frame of reference under the assumption of constant rotor speed, when in fact the rotor speed varies slightly within the prediction horizon. The violations are however relatively small compared to absolute values of the pitch rate limits and all in all the proposed method shows satisfactory performance.

VI. CONCLUSIONS AND FUTURE WORKS

The existing wind turbine control framework developed by the authors, consisting of an extended Kalman Filter and a Model Predictive Control algorithm as well as higher level functionality ensuring full wind speed range operation, has been extended to include multi-blade coordinate transformation in the control design model used by the control framework. The use of the multi-blade coordinate

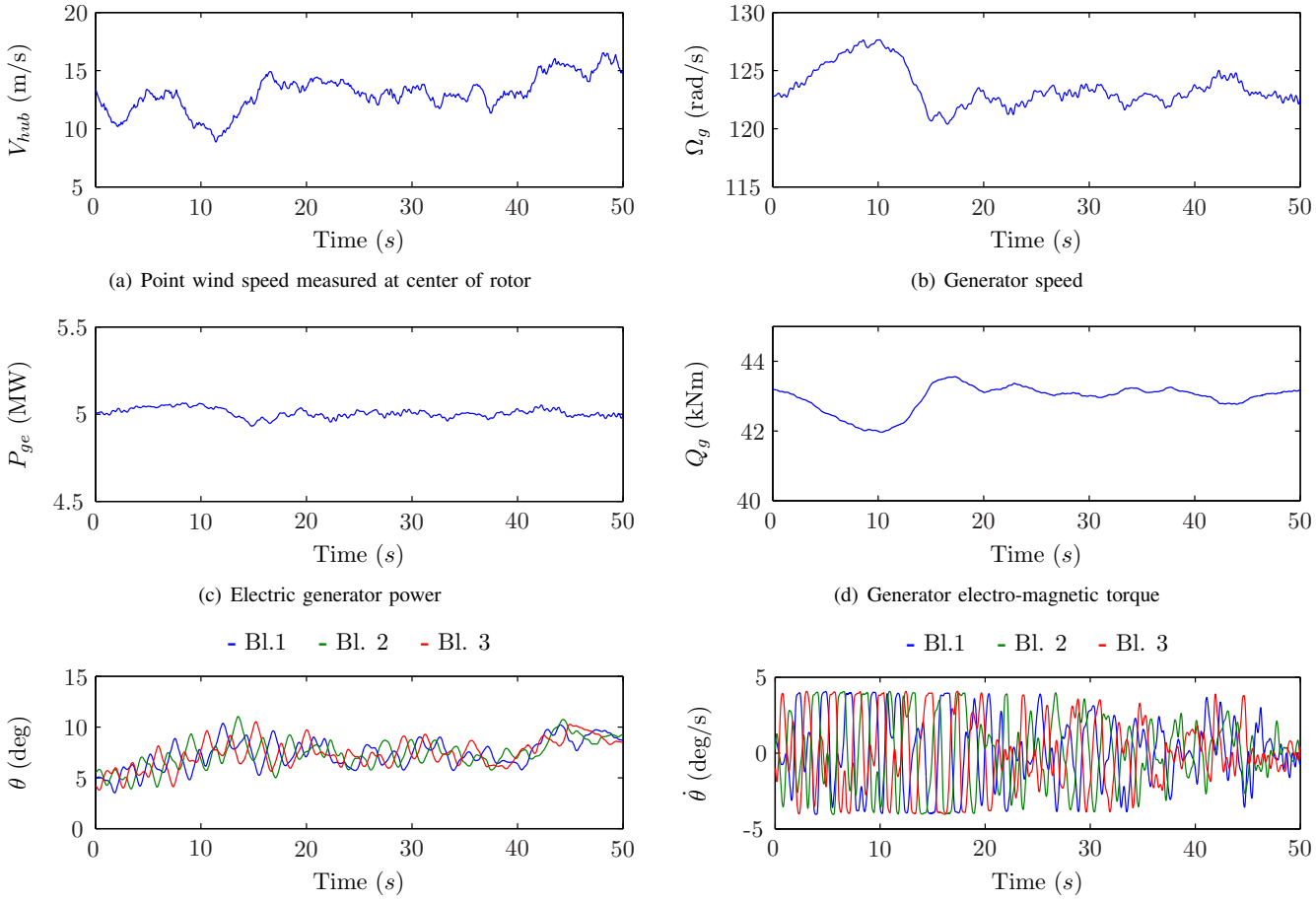

(a) Point wind speed measured at center of rotor

(b) Generator speed

(c) Electric generator power

(d) Generator electro-magnetic torque

(e) Individual pitch angles

(f) Individual pitch angle rates

Fig. 4. Simulation results at mean wind speed of 15 m/s. Pitch rate constrained to be within $\pm$ 4 deg/s.

transformation enables a more natural implementation of individual/cyclic pitch control which could lead to e.g. reduction in asymmetric loads caused by wind shear etc.

The Model Predictive Control algorithm has been extended such that constraints are still formulated in the rotating frame of reference although the rest of the system description is formulated in the fixed frame of reference. Numerical experiments performed in the aero-servo-elastic software HAWC2 confirms the controllers ability handle constraints on e.g. the pitch rate of individual blades.

In a broader perspective it would be relevant in future work to compare fatigue load reductions etc. achieved with the proposed method as opposed to alternative methods.

REFERENCES

[1] R. P. Coleman and A. M. Feingold. Theory of self-excited mechanical oscillations of helicopter rotors with hinged blades. Technical Report 1351, National Advisory Committee for Aeronautics (NACA), 1958.

[2] M. H. Hansen. Improved modal dynamics of wind turbines to avoid stall-induced vibrations. *Wind Energy*, 6(2):179–195, 2003.

[3] G. Bir. Multi-blade coordinate transformation and its application to wind turbine analysis. In *46th AIAA aerospace sciences meeting and exhibit*, Reno, NV., 2008. [CD ROM].

[4] K. Selvam, S. Kanev, J. W. van Wingerden, T. van Engelen, and M. Verhaegen. Feedback-feedforward individual pitch control for wind turbine load reduction. *International Journal of Robust and Nonlinear Control*, 19(1):72–91, 2009.

[5] S. C. Thomsen, N. K. Poulsen, and H. H. Niemann. Stochastic wind turbine control in multiblade coordinates. *Proc. Am. Control Conf., ACC*, pages 2772–2777, 2010.

[6] J. Richalet, A. Rault, J.L. Testud, and J. Papon. Model predictive heuristic control: Application to industrial processes. *Automatica*, 14(5):413–428, 1978.

[7] C.R. Cutler and B.L. Ramaker. Dynamic matrix control-a computer control algorithm. In *Proc. Joint Automatic Control Conf.*, pages Paper WP5–B, San Francisco, CA, 1980.

[8] L. C. Henriksen. *Model Predictive Control of Wind Turbines*. PhD thesis, Technical University of Denmark, Risø National Laboratory for Sustainable Energy, Wind Energy Division, 2010.

[9] L. C. Henriksen and N. K. Poulsen. An online re-linearization scheme suited for model predictive or linear quadratic control. IMM-Technical Report 2010-13, Dept. of Informatics and Mathematical Modelling, Technical University of Denmark, 2010.

[10] G. Pannocchia and J. B. Rawlings. Disturbance models for offset-free model-predictive control. *AIChE Journal*, 49(2):426–437, 2003.

[11] K. R. Muske and T. A. Badgwell. Disturbance modeling for offset-free linear model predictive control. *Journal of Process Control*, 12 (5):617–632, 2002.

[12] T. J. Larsen and A. M. Hansen. How 2 HAWC2, the user's manual. Technical Report Risø-R-1597(ver. 3-1)(EN), Risø National Laboratory, 2007.

[13] J. Mann. Wind field simulation. *Probabilistic Engineering Mechanics*, 13(4):269–282, 1998.

[14] J. Jonkman, S. Butterfield, W. Musial, and G. Scott. Definition of a 5-MW reference wind turbine for offshore system development. Technical Report NREL/TP-500-38060, National Renewable Energy Laboratory, 1617 Cole Boulevard, Golden, Colorado 80401-3393, February 2009.